11-2005

Effect of Chronic Hyperoxic Exposure on Duroquinone Reduction in Adult Rat Lungs

Said H. Audi
Marquette University, said.audi@marquette.edu

Robert D. Bongard
Medical College of Wisconsin

Gary S. Krenz
Marquette University, gary.krenz@marquette.edu

David A. Rickaby

Steven Thomas Haworth
Marquette University

See next page for additional authors

American Journal of Physiology : Lung Cellular and Moleculor Physiology, Vol. 289, No. 5 (2005): L788-797. DOI.

Effect of Chronic Hyperoxic Exposure on Duroquinone Reduction in Adult Rat Lungs

Said H. Audi
Marquette University
Robert D. Bongard
Concordia University Wisconsin
Gary S. Krenz
Marquette University
David A. Rickaby
Marquette University
Steven T. Haworth
Medical College of Wisconsin
Jessica Eisenhauer
Medical College of Wisconsin
David L. Roerig
Medical College of Wisconsin
Marilyn P. Merker
University of South Alabama

ABSTRACT

NAD(P)H:quinone oxidoreductase 1 (NQO1) plays a dominant role in the reduction of the quinone compound 2,3,5,6-tetramethyl-1,4-benzoquinone (duroquinone, DQ) to durohydroquinone (DQH_2) on passage through the rat lung. Exposure of adult rats to 85% O_2 for ≥7 days stimulates adaptation to the otherwise lethal effects of >95% O_2. The objective of this study was to examine whether exposure of adult rats to hyperoxia affected lung NQO1 activity as measured by the rate of DQ reduction on passage through the lung. We measured DQH_2 appearance in the venous effluent during DQ infusion at different concentrations into the pulmonary artery of isolated perfused lungs from rats exposed to room air or to 85% O_2. We also evaluated the effect of hyperoxia on vascular transit time distribution and measured NQO1 activity and protein in lung homogenate. The results demonstrate that exposure to 85% O_2 for 21 days increases lung capacity to reduce DQ to DQH_2 and that NQO1 is the dominant DQ reductase in normoxic and hyperoxic lungs. Kinetic analysis revealed that 21-day hyperoxia exposure increased the maximum rate of pulmonary DQ reduction, V_{max}, and the apparent Michaelis-Menten constant for DQ reduction, K_{ma}. The increase in V_{max} suggests a hyperoxia-induced increase in NQO1 activity of lung cells accessible to DQ from the vascular region, consistent qualitatively but not quantitatively with an increase in lung homogenate NQO1 activity in 21-day hyperoxic lungs. The increase in K_{ma} could be accounted for by ∼40% increase in vascular transit time heterogeneity in 21-day hyperoxic lungs.

Pulmonary oxidative stress has been implicated in the pathogenesis of many acute and chronic pulmonary inflammatory diseases[12, 15, 16, 20]. Several animal models of hyperoxic lung injury have been developed to investigate the underlying mechanisms of pulmonary oxygen toxicity and the lung response to oxidative stress[12–15, 20, 26, 32, 33]. Exposure of an adult rat to >95% O_2 results in lung injury within 48–60 h and death within 72 h[14, 15]. Adult rats exposed to 85% O_2 also develop lung injury within 48–72 h, but unlike other species, including mice, guinea pigs, and hamsters, they survive the initial lung injury, and after 7 or more days of exposure to 85% O_2, they develop tolerance or adaptation to otherwise lethal hyperoxia (>95% O_2) [14, 15]. Although the activities of the so-called classic antioxidant enzymes such as superoxide dismutase and catalase are increased in rats adapted to lethal hyperoxia[14, 15, 21], they do not appear to account for all aspects of this adaptive response[13, 20, 32].

Another proposed mechanism involved in rat adaptation to lethal hyperoxia is the induction of phase II detoxification enzymes including NAD(P)H:quinone oxidoreductase 1 (NQO1), glutathione-*S*-transferase, and heme oxygenase-1[12, 26]. The induction occurs via the antioxidant response element mediated by enhanced production of reactive oxygen species[12, 26]. Phase II enzymes are, in general, involved in detoxification of reactive electrophilic metabolites including organic peroxides, lipid peroxides, and quinones via conjugation reactions or two-electron reduction that enhance their excretion[9, 12, 17]. With respect to NQO1, it has been suggested that additional protective effects include regeneration of endogenous and exogenous antioxidants[8, 17, 31], competition with one-electron quinone reductases, thereby ameliorating the effects of semiquinone formation and subsequent redox cycling[9, 33], and scavenging superoxide[30].

The model quinone, duroquinone (DQ), is one of several redox active compounds that we have used to probe pulmonary endothelial surface and intracellular redox enzymes in the intact lung using indicator dilution methods[1, 2, 4, 6]. We have demonstrated that NQO1 plays a dominant role in DQ reduction to its

two-electron reduction product durohydroquinone (DQH_2) on a single pass through the rat pulmonary circulation[1]. The present study examines whether exposure of adult rats to hyperoxia (85% O_2 for 48 h or 21 days) affects NQO1 activity in the intact rat lung as measured by the rate of DQ reduction on passage through the lungs. The main approach we took was to measure the rate of appearance of DQH_2 in the venous effluent during DQ infusion at different concentrations into the pulmonary artery of isolated perfused lungs from normal rats and from rats that had been exposed to 85% O_2 for 48 h or 21 days. We also evaluated the effect of rat exposure to hyperoxia on vascular transit time heterogeneity and measured NQO1 protein and activity in lung homogenate. The results demonstrate increased DQ reduction capacity in lungs of rats exposed to hyperoxia for 21 days and provide insight into the effects of hyperoxia-induced increase in pulmonary vascular transit time heterogeneity on steady-state Michaelis-Menten kinetics.

METHODS

Materials

DQ was purchased from Sigma Chemical (St. Louis, MO). Bovine serum albumin (BSA, standard powder) was purchased from Serologicals (Gaithersburg, MD). DQH_2 was prepared by reduction of DQ with potassium borohydride (KBH_4) as previously described[10]. Other chemicals were purchased from Sigma Chemical and were of reagent grade.

Hyperoxic Exposure

Adult Sprague-Dawley rats (Charles River; 250–350 g) were housed in a sealed Plexiglas chamber (13-inch width × 23-inch length × 12-inch height) with ~85% O_2 balance N_2 for 48 h [final body wt, 326 ± 5 (SE) g, $n = 10$] or 21 days (final body wt, 290 ± 8 g, $n = 14$). The total gas flow of ~3.5 l/min was high enough to maintain the chamber CO_2 at <0.5%. The animals were maintained on a 12-h light-dark cycle with free access to food and water, which along with bedding, were changed every other day. Control (normoxic) animals (final body wt, 324 ± 6 g, $n = 21$) were exposed to room air. The protocol was approved by the Institutional Animal Care and Use Committees of the Veterans Affairs Medical Center and Marquette University (Milwaukee, WI).

The 48-h exposure period was chosen to evaluate hyperoxia-induced changes in lung DQ reduction rate and lung NQO1 protein and activity before the development of tolerance to lethal hyperoxia (>95% O_2) [14, 15]. The 21-day exposure period was chosen because it is long enough to stimulate adaptation to >95% O_2 [14, 15] and to reverse the body weight loss that occurs during the first 2 wk of exposure to 85% O_2 [14]. Lungs of control rats will be referred to as normoxic lungs, and lungs of rats exposed to hyperoxic gas mixture for 48 h or 21 days as 48-h hyperoxic lungs and 21-day hyperoxic lungs, respectively.

Isolated Perfused Lung Experiments

The isolated perfused rat lung preparation has been described previously[1]. Briefly, each rat was anesthetized with pentobarbital sodium (40 mg/kg body wt ip), after which the trachea was clamped and the chest opened. Heparin (0.7 IU/g body wt) was injected into the right ventricle. The pulmonary artery and the trachea were cannulated, and the pulmonary venous outflow was accessed via a cannula in the left atrium. The lungs were removed from the chest and attached to a ventilation and perfusion system. The perfusate (referred to as control perfusate) was a physiological salt solution

containing (in mM) 4.7 KCl, 2.51 $CaCl_2$, 1.19 $MgSO_4$, 2.5 KH_2PO_4, 118 NaCl, 25 $NaHCO_3$, 5.5 glucose, and 5% BSA[1].

The single pass perfusion system was primed with control perfusate maintained at 37°C and equilibrated with 15% O_2, 6% CO_2, balance N_2 resulting in perfusate Po_2, Pco_2, and pH of ~105 Torr, 40 Torr, and 7.4, respectively. Initially, perfusate was pumped (Master Flex roller pump) through the lungs until the lungs were evenly blanched and venous effluent was visually clear of blood. The flow rate was then set at 10 ml/min. The lungs were ventilated (40 breaths/min) with end inspiratory and expiratory pressures of 6 and 3 mmHg, respectively, with the above gas mixture. The pulmonary arterial pressure was referenced to atmospheric pressure at the level of the left atrium and monitored continuously during the course of the experiments. The venous effluent pressure was atmospheric pressure. At the end of each experiment, the lungs were weighed and then dried (60°C) to a constant weight to determine lung dry weight and wet/dry weight ratio. For some lungs, half was homogenized for in vitro determination of NQO1 protein and activity as described below, and the other half was used to determine lung dry weight and wet/dry weight ratio.

To measure the fate of DQ on passage through the lungs, pulse infusion and bolus injection experiments were carried out[1]. The pulse infusion experiments provide data in which information about the steady-state aspects of DQ and DQH_2 disposition on passage through the lungs is emphasized, whereas the bolus experiments provide data in which information about the transient aspects of DQ and DQH_2 disposition is emphasized.

Experimental Protocols

Capacity of lungs for DQ reduction.

To determine the DQ reducing capacity of normoxic and hyperoxic lungs, four 60- to 90-s sequential pulse infusions at DQ concentrations of 50, 100, 200, and 400 µM were carried out on each lung. The pump flow rate was set at 10 ml/min. For each pulse infusion, venous effluent samples (~0.5 ml) were collected at 10-s intervals during infusion. Between pulse infusions, the lungs were perfused with ~20 ml of fresh perfusate to wash the perfusion system and the lungs of any remaining traces of DQ and/or DQH_2 from the previous pulse. Multiple DQ pulses and high DQ concentrations did not have a significant effect on DQ reduction in subsequent pulses[1].

Inhibitor treatments.

To determine the contribution of NQO1 to DQ reduction in normoxic and hyperoxic lungs, DQ pulse infusions were carried out before and after lung treatment with the NQO1 inhibitor dicumarol[25]. For each lung, a 90-s pulse infusion of 400 µM DQ was performed, and venous samples were collected as before. This was followed by perfusing the lung with perfusate containing dicumarol (400 µM) for ~5 min. After treatment with dicumarol, another 90-s pulse infusion of DQ (400 µM) plus dicumarol (400 µM) was performed, and venous samples were collected as before. The above concentration of dicumarol was needed to inhibit lung NQO1 activity because dicumarol has a high affinity for plasma proteins[34].

To determine the contribution of DQH_2 oxidation to the net effect of the lung on DQ, the above pulse infusion protocol used to determine capacity of lungs for DQ reduction, was repeated in lungs pretreated with cyanide (2 mM)[1]. This was accomplished by recirculating perfusate containing cyanide

(2 mM) through the lungs for 5 min, a dose and time previously determined to be sufficient to inhibit DQH_2 oxidation to DQ on passage through the lungs[1].

Bolus injections.

Bolus injection experiments were carried out to evaluate hyperoxia-induced changes in lung tissue volume accessible to DQH_2 from the vascular space, lung vascular volume, and vascular perfusion heterogeneity. An injection loop was included in the arterial line to allow introduction of a 0.1-ml bolus into the arterial inflow without altering the flow or perfusion pressure[1]. For each lung, perfusate containing cyanide (2 mM) was recirculated for 5 min just before bolus injection. The pump flow rate was set at 10 ml/min. The respirator was stopped at end expiration, and a bolus of the perfusate solution containing either 400 μM DQH_2 or 35 μM of the vascular reference indicator fluorescein isothiocyanate dextran (FITC-dex; average mol wt ~43,000) was injected. At the same time that the bolus was introduced into the arterial inflow, the venous outflow was diverted into a modified Gilson Escargot fraction collector for continuous collection of the lung effluent[1]. Thirty-five venous effluent samples (0.3 ml each) were collected at 1.8-s intervals. At the end of each experiment, the lungs were removed from the perfusion system, the arterial and venous cannulas were connected directly together, and an additional FITC-dex bolus injection was made. These data were used to obtain the tubing transit time and bolus dispersion needed for calculation of the lung vascular volume and the relative dispersion of vascular transit time distribution (see *Data Analysis*).

Perfused capillary surface area.

To evaluate hyperoxia-induced changes in pulmonary endothelial surface area, the rate of hydrolysis of the peptide *N*-[3-(2-furyl)acryloyl]-Phe-Gly-Gly (FAPGG), an angiotensin converting enzyme (ACE) substrate, on a single pass through the pulmonary circulation was measured[27]. To establish the linearity of the steady-state rate of FAPGG hydrolysis as a function of FAPGG concentration, three pulse infusions with sequentially increasing FAPGG concentrations (100, 200, and 300 μM) were carried out in a normoxic lung. During each infusion, the flow rate was set at 30 ml/min, and venous effluent samples were collected 20 s after the start of the infusion period, which is long enough for the venous FAPGG concentration to reach steady state. For all other normoxic and hyperoxic lungs studied, two 150-μM FAPGG pulse infusions were carried out at the beginning and at the end of each of the above experimental protocols, and venous samples were collected as before. This concentration was determined to fall within the linear range for the steady-state rate of FAPGG hydrolysis on passage through the lungs (see results). A permeability-surface area product (PS; ml/min), as a measure of the rate constant of ACE-mediated FAPGG hydrolysis on passage through the lungs and an index of perfused capillary surface area, was calculated from the infused arterial FAPGG concentration ($[FAPGG]_i$) and steady state venous effluent FAPGG concentration ($[FAPGG]_o$) using

$$\mathrm{PS} = -\mathrm{F}\ln(1-\mathrm{E})$$

(1)

$$\text{where E=steady - state exteraction ratio} = 1 - \frac{[\mathrm{FAPGG}]_o}{[\mathrm{FAPGG}]_i}$$

(2)

and F is the perfusate flow rate (30 ml/min).

Determination of DQ, DQH_2, and FITC-Dex Concentrations in Venous Effluent Samples

The concentrations (in μM) of DQ and DQH_2 in the venous effluent samples were determined as previously described[1]. Briefly, the venous effluent samples were centrifuged (1.0 min at 5,600 *g*), after which for each sample 100 μl of the supernatant was pipetted into each of two microcentrifuge tubes, one containing 10 μl of deionized water, and the other containing 10 μl of potassium ferricyanide (1.8–7.2 mM) to oxidize any DQH_2 contained in the sample to DQ. Ice-cold absolute ethanol (0.4–0.8 ml) was added to each tube, and the tubes were centrifuged at 5,600 *g* for 5 min at 4°C. DQ and DQH_2 concentrations (in μM) were measured spectrophotometrically at 265 nm using molar extinction coefficients of 21,640 $M^{-1}cm^{-1}$ for DQ and 1,700 $M^{-1}cm^{-1}$ for DQH_2. FITC-dex concentrations in the venous effluent samples were measured spectrophotometrically at 495 nm using a molar extinction coefficient of 93,478 $M^{-1}cm^{-1}$. In addition, for the bolus experiments, measured volumes of the injected bolus were added to samples that emerged in the venous effluent before the appearance of the bolus contents. These samples were used as standards for determining the fraction of bolus contents per milliliter of venous effluent sample.

Lung Homogenate NQO1 Activity and NQO1 Immunoblots

At the end of the DQ reduction studies that did not involve using metabolic inhibitors, the lungs were removed from the perfusion system, weighed, and placed on ice. Ice-cold homogenization buffer (5 ml of buffer/g of lung tissue, pH 7.4) containing (in mM) 10 HEPES, 250 sucrose, 3 EDTA, 1 phenylmethylsulfonyl fluoride, and 1% protease inhibitor cocktail (Sigma, cat. no. P8340) was added. The lungs were minced and homogenized on ice using a Polytron tissue homogenizer. The resulting lung homogenate was centrifuged (12,100 *g*) at 4°C for 30 min. The supernatant was collected and stored on ice, and the protein concentration was determined (Bio-Rad Laboratories, Hercules, CA) using BSA as the standard.

Whole lung NQO1 activity was measured using a modified procedure of Lind et al.[22]. Lung homogenate supernatant protein (~10 μg) was added to a semimicro cuvette containing 1 ml of reaction buffer that consisted of Tris·HCl (25 mM, pH 7.4), BSA (0.23 mg/ml), Tween 20 (0.01% vol/vol), 2,6-dichlorophenolindophenol (DCIP, 50 μM), and flavin adenine dinucleotide (5 μM) with and without dicumarol (20 μM). The reaction was initiated by the addition of NADPH (final concentration 200 μM). DCIP reduction (extinction coefficient 21,000 $M^{-1}cm^{-1}$) was measured spectrophotometrically at 600 nm (25°C). The NQO1 activity was calculated as the difference in the initial rates of DCIP reduction in the absence and presence of dicumarol (20 μM)[23, 33].

To determine the effect of hyperoxic exposure on lung NQO1 protein expression, immunoblot analysis was carried out as previously described[1]. A portion of the lung homogenate supernatant (37.5 μg of protein) and purified recombinant human NQO1 protein (0.25 ng) were subjected to electrophoresis using NuPAGE LDS sample buffer (Invitrogen, Carlsbad, CA), 4–12% gradient NuPAGE Bis-Tris gel, and MES-SDS running buffer, as previously described[1, 24]. The proteins were transferred to a nitrocellulose membrane that was incubated for 1 h in Tris-buffered saline containing 0.1% Tween 20 and 2% BSA, the latter as a blocking agent. The membrane was then incubated sequentially in a 1:10 dilution of tissue culture supernatant containing anti-NQO1 monoclonal antibodies (IgG_1) from two mouse

hybridoma cell lines (A180 and B771, mixed 1:1; a gift of Dr. David Siegel, Univ. of Colorado Heath Sciences Center, Denver, CO), a 1:7,500 dilution of goat α-mouse IgG-horseradish peroxidase (Jackson ImmunoResearch Laboratories), and the Supersignal West Pico Chemiluminescent substrate (Pierce). The signal was captured on CL-Xposure Film (Pierce). As a control, nonspecific mouse IgG_1 was substituted for the α-NQO1 monoclonal antibodies. Densitometry was used to quantify band intensities.

Statistical Evaluation of Data

Statistical comparisons among the various experimental conditions were obtained by ANOVA followed by Dunnett's test. $P < 0.05$ was considered statistically significant.

RESULTS

Table 1 shows perfusion pressures, wet weights, dry weights, and wet/dry weight ratios of the lungs studied. Exposure to hyperoxia for 21 days increased lung perfusion pressure and wet and dry weights, with small (<9%) but significant increase in wet/dry weight ratios compared with normoxic lungs, indicating a slight edema in hyperoxic lungs. Exposure to hyperoxia for 48 h had no significant effect on any of the above parameters or on any of the parameters described below. Thus the results presented below are limited to comparisons between normoxic lungs and 21-day hyperoxic lungs.

Table 1. Lung weights and perfusion pressures

	P_a, Torr	Wet Wt, g	Dry Wt, g	Wet/Dry Ratio
Normoxia	6.1±0.2	1.29±0.03	0.230±0.004	5.6±0.1
Hyperoxia, 48 h	6.1±0.3	1.28±0.06	0.229±0.004	5.6±0.2
Hyperoxia, 21 days	13.7±0.7*	2.36±0.10*	0.384±0.012*	6.1±0.2*

Values are means ± SE. P_a is the lung perfusion pressure with the pump flow rate set at 10 ml/min; $n = 21$, 10, and 14 for normoxic lungs, 48-h hyperoxic lungs, and 21-day hyperoxic lungs, respectively.
*Significantly different from the normoxic value.

Lung's DQ Reducing Capacity

Figure 1*A* shows the effluent concentrations of DQ and DQH_2 (as fractions of the total effluent [DQ] + [DQH_2]) vs. sampling time obtained during a pulse infusion of 100 μM DQ in a normoxic lung perfused with control perfusate. The venous effluent [DQ] and [DQH_2] reached a steady state by ~50 s. Figure 1*B* shows the fractional steady-state [DQ] and [DQH_2] in the venous effluent of a normoxic lung during DQ infusion, expressed as the average of their respective concentrations in samples collected 60 s after the start of DQ infusion. As the infused [DQ] increased, the fractional steady-state [DQ] increased, whereas that of [DQH_2] decreased.

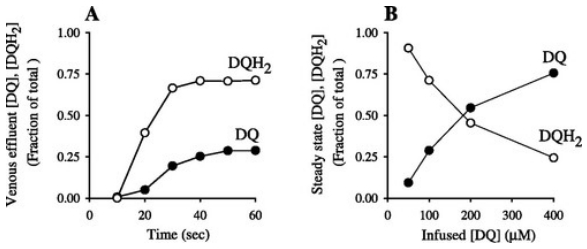

Fig. 1.*A*: example of the time course for the venous effluent concentrations (as fractions of the respective total effluent [DQ] + [DQH_2]) of duroquinone (DQ) and durohydroquinone (DQH_2) during a pulse infusion of 100 μM

DQ into the pulmonary artery of a normoxic lung perfused with control perfusate at 10 ml/min. *B*: steady-state venous effluent [DQ] and [DQH_2] during DQ infusion at 50, 100, 200, or 400 μM into the pulmonary artery of a normoxic lung perfused with control perfusate at 10 ml/min. Steady-state venous effluent [DQ] and [DQH_2] were calculated as the average of their concentrations in samples collected after 60 s of DQ infusion.

Table 2 summarizes the DQ pulse infusion steady-state data obtained using control perfusate. The 21-day hyperoxic lungs had a higher steady-state venous effluent [DQH_2] than normoxic lungs during the infusion of DQ at 200 and 400 μM.

Table 2. Steady-state effluent [DQH_2] during DQ infusion in lungs perfused with control perfusate or perfusate containing dicumarol

Infused [DQ]	**Steady-State Effluent [DQH_2], μM**		
	Normoxia	**Hyperoxia, 48 h**	**Hyperoxia, 21 days**
50 μM	37.8±1.3	41.2±1.2	36.0±0.7
100 μM	64.2±2.4	70.3±2.2	66.9±2.3
200 μM	95.7±4.9	99.0±6.6	112±2.1*
400 μM	99.8±4.5	107±5.8	150±4.7*
400 μM + Dicumarol	2.1±1.0†	3.5±0.6†	2.9±1.9†

Values are means ± SE; $n = 7$, 4, and 5 for normoxic lungs, 48-h hyperoxic lungs, and 21-day hyperoxic lungs, respectively. For 400 μM pulse infusions, $n = 12$, 7, and 8 for normoxic lungs, 48-h hyperoxic lungs, and 21-day hyperoxic lungs, respectively. For 400 μM pulse infusions + dicumarol (400 μM), $n = 5$, 3, and 3 for normoxic lungs, 48-h hyperoxic lungs, and 21-day hyperoxic lungs, respectively.
*Significantly different from the normoxic value.
†Significantly different from 400 μM duroquinone (DQ) without dicumarol. DQH_2, durohydroquinone.

Inhibitor Treatments

To evaluate the contribution of NQO1 to DQ reduction, we examined the effect of dicumarol, an NQO1 inhibitor, on DQ reduction[1, 25]. Table 2 shows that dicumarol almost completely (>96%) inhibited reduction of 400 μM DQ pulse infusion in normoxic and hyperoxic lungs.

Table 3 summarizes the steady-state venous effluent [DQH_2] measured during DQ infusion in normoxic and hyperoxic lungs in the presence of cyanide (2 mM), which blocks DQH_2 oxidation to DQ[1]. Compared with studies in control perfusate (Table 2), the steady-state venous effluent [DQH_2] increased at all four DQ concentrations studied in normoxic lungs and 21-day hyperoxic lungs. Table 3 also shows that cyanide increased steady-state venous effluent [DQH_2] during infusion of 400 μM DQ in 21-day hyperoxic lungs compared with normoxic lungs.

Table 3. Steady-state effluent [DQH_2] during DQ infusion in lungs perfused with control perfusate containing 2 mM cyanide

Infused [DQ] + cyanide, μM	**Steady-State Effluent [DQH_2], μM**		
	Normoxia	**Hyperoxia, 48 h**	**Hyperoxia, 21 days**
50	43.2±1.3	43.9±1.6	42.7±0.8
100	81.4±2.1	75.0±2.1	74.8±1.7
200	132±1.5	128±4.6	143±4.9
400	161±6.7	170±11.8	221±11.0*

Values are means ± SE; $n = 4$, 3, and 4 for normoxic lungs, 48-h hyperoxic lungs, and 21-day hyperoxic lungs, respectively.
*Significantly different from the normoxic value.

The difference in the steady-state venous effluent [DQH_2] during DQ infusion with and without cyanide (Δ[DQH_2]) is proportional to DQH_2 oxidation rate. Because DQ pulse infusions with and without cyanide were not carried out in the same lungs, Δ[DQH_2] was approximated as the difference between the steady-state venous effluent [DQH_2] during DQ infusion in the absence of cyanide and the corresponding mean steady-state venous effluent [DQH_2] values in the presence of cyanide (Table 3). Figure 2 shows a linear relationship between Δ[DQH_2] and the infused [DQ] and that this relationship (as measured by the slope of Δ[DQH_2] vs. infused [DQ]) was not significantly affected by exposure to hyperoxia.

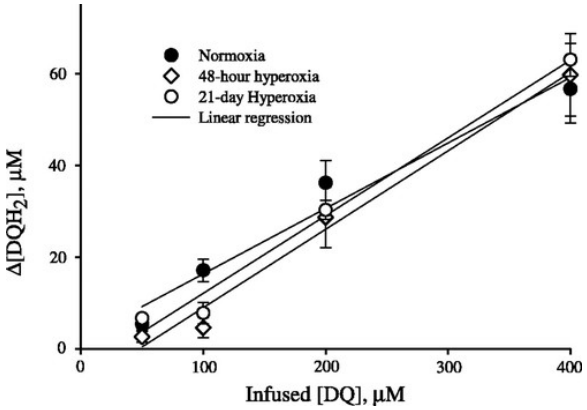

Fig. 2. Differences in the steady-state venous effluent [DQH_2] during DQ infusion in the presence and absence of cyanide, Δ[DQH_2], are plotted vs. infused [DQ]. Values are means ± SE, $n = 7$, 4, and 5 for normoxic lungs, 48-h hyperoxic lungs, and 21-day hyperoxic lungs, respectively. Solid lines are linear regression fit to the data.

Bolus Injections

Figure 3 shows examples of venous effluent concentrations of FITC-dex, DQ, and DQH_2 after bolus injections of DQH_2 and FITC-dex in a normoxic lung (Fig. 3*A*) and a 21-day hyperoxic lung (Fig. 3*B*). The lungs were treated with cyanide (2 mM) before the bolus injection to inhibit DQH_2 oxidation to DQ. Little or no DQ was detected in the venous effluent following the bolus injection of DQH_2, consistent with cyanide inhibition of tissue-mediated DQH_2 oxidation and the reported slow DQH_2 autooxidation rate[1]. The FITC-dex concentration vs. time curve indicates what the effluent DQH_2 curve would have been had the DQH_2 not interacted with the lung as it passed through the pulmonary vessels. The DQH_2 curves for normoxic lung and 21-day hyperoxic lung (Fig. 3) are shifted to the right and more dispersed than the FITC-dex curves, consistent with a flow-limited distribution of DQH_2 into the tissue[1].

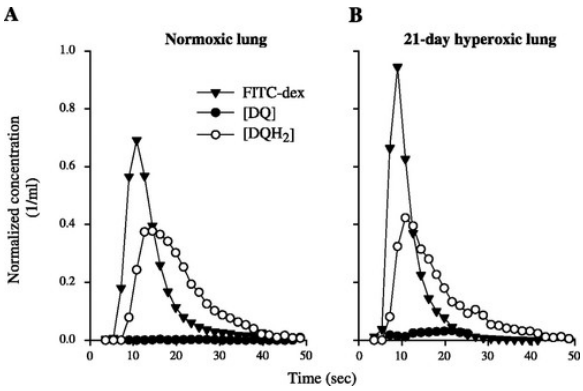

Fig. 3. Venous effluent concentration (as a fraction of injected amount per milliliter of effluent perfusate) vs. time curves for FITC-dextran, DQ, and DQH_2 following the bolus injection of FITC-dextran and DQH_2 into the pulmonary artery of a normoxic lung (*A*) and a 21-day hyperoxic lung (*B*). The lungs had been treated with cyanide (2 mM) before the bolus injection to inhibit DQH_2 oxidation to DQ.

Perfused Capillary Surface Area

The steady-state rate of FAPGG hydrolysis in a normoxic lung perfused with control perfusate was linear over a wide range of FAPGG concentrations that included the concentration (150 μM) used in the present study to calculate a PS for ACE-mediated FAPGG hydrolysis. Table 4 shows that exposure to hyperoxia for 21 days decreased PS (ml/min) on average by >70% compared with normoxic lungs. The PS values obtained from FAPGG pulse infusions carried out at the beginning or at the end of a given experimental protocol were not significantly different, indicating that perfusion, multiple DQ pulses, and/or metabolic treatments did not have significant irreversible effects on lung capillary endothelial surface area and/or ACE activity.

Table 4. Lung angiotensin converting enzyme activity, vascular volumes, and DQH_2 extravascular volumes and perfusion heterogeneity

	PS, ml/min	Q_V, ml	Q_D, ml	RD_V
Normoxia	21.8±1.0	0.75±0.05	1.15±0.04	0.71±0.06
Hyperoxia, 48 h	25.0±1.0	0.64±0.03	1.20±0.10	0.70±0.02
Hyperoxia, 21 days	5.8±0.4*	0.52±0.05*	1.29±0.13	1.01±0.08*

Values are means ± SE. PS, permeability surface area product, is a measure of angiotensin converting enzyme-mediated FAPGG hydrolysis; Q_V and Q_D are the lung vascular volume and DQH_2 extravascular volume, respectively. RD_V is the relative dispersion of vascular transit time distribution. For PS, $n = 20$, 10, and 14 for normoxic lungs, 48-h hyperoxic lungs, and 21-day hyperoxic lungs, respectively. For Q_V and Q_D, $n = 3$ for all three sets of lungs.

*Significantly different from the normoxic value.

Effect of Hyperoxia on NQO1 Activity and Protein

Table 6 shows that exposure to hyperoxia for 21 days significantly increased NQO1 activity in lung homogenate by ~34% compared with normoxic lungs on a per milligram protein basis.

Figure 4 shows NQO1 immunoblots of normoxic and hyperoxic lung homogenates. Band intensities obtained from 21-day hyperoxic lung homogenates were, on average, more than threefold greater than those from normoxic lung homogenates.

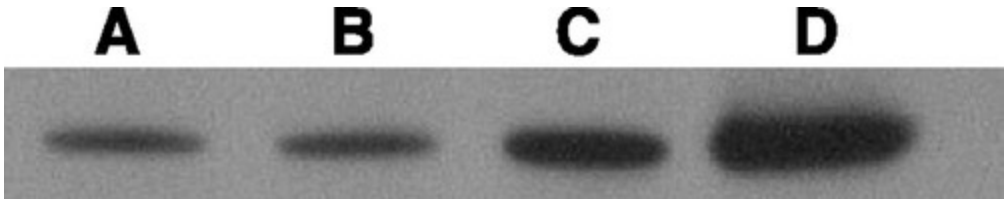

Fig. 4. NAD(P)H:quinone oxidoreductase 1 (NQO1) immunoblots in lung tissue from a normoxic (*A*) rat and from rats that had been exposed to hyperoxia for 48 h (*B*) or 21 days (*C*). Human recombinant NQO1 (0.25 ng of protein) was used as a standard (*D*). There were no detectable corresponding bands in the same region of the blots when control, nonspecific IgG1 was used in place of α-NQO1 antibody. The NQO1 immunoblots shown were chosen for illustrative purposes since their band densities are close to their respective mean values. Band intensities were 2.0 ± 0.3 SE ($n = 9$) for normoxic lungs, 2.6 ± 0.4 ($n = 9$) for 48-h hyperoxic lungs, and 6.1 ± 1.4 ($n = 5$) for 21-day hyperoxic lungs.

Data Analysis

Kinetic model.

To interpret the experimental results, a kinetic model previously described[1] was modified to describe the fate of DQ on passage through the lungs. The model consists of a capillary volume (V_c) and its surrounding tissue volume (V_e). The free forms (i.e., not albumin bound) of both DQ and DQH_2 are assumed to be freely permeable into V_e[1]. Within V_c, the model allows for nonspecific rapidly equilibrating interactions of DQ and DQH_2 with the perfusate albumin (P_c) (*Eq. 3*). Within V_e, the model allows for two-electron DQ reduction to DQH_2 (*Eq. 4*), cyanide-sensitive DQH_2 oxidation to DQ (*Eq. 5*), and nonspecific rapidly equilibrating interactions of DQ and DQH_2 with lung tissue sites of association (P_e) (*Eq. 6*). The reduction of DQ to DQH_2 is assumed to follow Michaelis-Menten kinetics, where V_{max} and K_m represent the maximum reduction rate and the Michaelis-Menten constant, respectively. All other reactions are assumed to follow the law of mass action and to proceed with a rate constant k_i in the forward direction and, if reversible within the time course of the study, with a rate constant k_{-i} in the reverse direction. Each of the stoichiometric equations may potentially represent multiple parallel and/or series processes that are not explicitly specified. For example, intracellular reduction might occur via parallel enzymes, with different V_{max} and K_m for DQ, contributing to the total quinone reductase activity.

In perfusate

$$\text{perfusate albumin, } P_c\text{, association } DQ + P_c \underset{k_{-1}}{\overset{k_1}{\rightleftarrows}} DQ - P_c \quad DQH_2 + P_c \underset{k_{-1}}{\overset{k_1}{\rightleftarrows}} DQH_2 - P_c$$

(3)

In tissue

$$\text{Reduction } DQ + EH + H^+ \xrightarrow{V_{max}, K_m} DQH_2 + E^+$$

(4)

$$\text{Oxidation} \quad DQH_2 + \frac{1}{2}O_2 \xrightarrow{k_3} H_2O + DQ$$

(5)

$$\text{Rapidly equilibrating associations } \mathrm{DQ} + \mathrm{P_e} \underset{k_{-4}}{\overset{k_4}{\rightleftarrows}} \mathrm{DQ-P_e} \quad \mathrm{DQH_2} + \mathrm{P_e} \underset{k_{-5}}{\overset{k_5}{\rightleftarrows}} \mathrm{DQH_2-P_e}$$

(6)

where EH and E^+ are the reduced and oxidized forms, respectively, of intracellular electron donor(s), and the k_is represent the reaction rate constants.

The above stoichiometric relationships are expressed as species balance equations

$$\frac{\partial[\mathrm{R}]}{\partial \mathrm{t}} + \mathrm{W}\frac{\partial[\mathrm{R}]}{\partial \mathrm{x}} = 0$$

(7)

$$\frac{\partial[\mathrm{D}\overline{\mathrm{Q}}]}{\partial \mathrm{t}} + \mathrm{W}\left(\frac{\mathrm{V_c}}{\mathrm{V_c} + \frac{\mathrm{V_{F1}}}{\alpha_1}}\right)\frac{\partial[\mathrm{D}\bar{\mathrm{Q}}]}{\partial \mathrm{x}} = \left(\frac{[\mathrm{D}\bar{\mathrm{Q}}\mathrm{H_2}]}{\mathrm{V_c} + \frac{\mathrm{V_{F1}}}{\alpha_1}}\right)\left(\frac{k_0}{\alpha_3}\right) - \left(\frac{[\mathrm{D}\bar{\mathrm{Q}}]}{\mathrm{V_c} + \frac{\mathrm{V_{F1}}}{\alpha_1}}\right)\left(\frac{V_{\max}}{K_{\mathrm{ma}} + [\mathrm{D}\overline{\mathrm{Q}}]}\right)$$

(8)

$$\frac{\partial[\mathrm{D}\overline{\mathrm{QH_2}}]}{\partial \mathrm{t}} + \mathrm{W}\left(\frac{\mathrm{V_c}}{\mathrm{V_c} + \frac{\mathrm{V_{F2}}}{\alpha_3}}\right)\frac{\partial[\mathrm{D}\bar{\mathrm{Q}}\mathrm{H_2}]}{\partial \mathrm{x}} = -\left(\frac{[\mathrm{D}\bar{\mathrm{Q}}\mathrm{H_2}]}{\mathrm{V_c} + \frac{\mathrm{V_{F2}}}{\alpha_3}}\right)\left(\frac{k_0}{\alpha_3}\right) - \left(\frac{[\mathrm{D}\bar{\mathrm{Q}}]}{\mathrm{V_c} + \frac{\mathrm{V_{F2}}}{\alpha_3}}\right)\left(\frac{V_{\max}}{K_{\mathrm{ma}} + [\mathrm{D}\overline{\mathrm{Q}}]}\right)$$

(9)

where W = convective transport velocity = $\mathrm{L}/\bar{\mathrm{t}}_c$; $x = 0$ and $x = L$ are the capillary inlet and outlet, respectively; $\bar{\mathrm{t}}_c$ is the capillary mean vascular transit time; [R](x, *t*) is the concentration of the vascular reference indicator (FITC-dex) at distance x from the capillary inlet and time *t*; [DQ](x, *t*) and [DQH_2](x, *t*) are vascular concentrations of free DQ and DQH_2 forms, respectively, [$D\bar{Q}$] at distance x from the capillary inlet and time *t*; [$D\bar{Q}$] = ([DQ]$\bar{\alpha}_1$) and [DQH2] = ([DQH_2]α_3) are the total (free + protein bound) vascular concentrations of DQ and DQH_2, respectively; $\alpha_1 = 1 + [P_c]\, k_1/k_{-1}$ and $\alpha_3 = 1 + [P_c]\, k_2/k_{-2}$ are constants that account for the rapidly equilibrating interactions of DQ and DQH_2 with perfusate BSA. $K_{ma} = \alpha_1 K_m$ (μM) is the apparent Michaelis-Menten constant; $V_{F1} = \alpha_2 V_e$ and $V_{F2} = \alpha_4 V_e$ (ml) are the virtual volumes of distribution, where $\alpha_2 = 1 + [P_e]\, k_4/k_{-4}$ and $\alpha_4 = 1 + [P_e]\, k_5/k_{-5}$ are constants that account for the rapidly equilibrating interactions of DQ and DQH_2 with lung tissue sites of association, respectively; $k_o = V_e\, k_3 [O_2]^{1/2}$ (ml·min^{-1}) is the tissue-mediated DQH_2 oxidation rate constant. To put k_o in perspective, if one were to assume Michaelis-Menten kinetics for DQH_2 oxidation, k_o would be an approximation to the ratio of the maximum oxidation rate over the Michaelis-Menten constant. The [H^+], [O_2], and [EH] included in some parameter groups are assumed constant during a given sample collection period[1].

For the steady state during the pulse infusion of DQ or DQH_2, *Eqs. 8* and *9* reduce to

$$\mathrm{WV}_c\frac{\partial[\mathrm{D}\bar{\mathrm{Q}}]}{\partial \mathrm{x}} = [\mathrm{D}\bar{\mathrm{Q}}\mathrm{H_2}]\left(\frac{k_0}{\alpha_3}\right) - [\mathrm{D}\bar{\mathrm{Q}}]\left(\frac{V_{\max}}{K_{\mathrm{ma}} + [\mathrm{D}\overline{\mathrm{Q}}]}\right)$$

(10)

$$\mathrm{WV}_c \frac{\partial[\mathrm{D\bar{Q}H_2}]}{\partial \mathrm{x}} = [\mathrm{D\bar{Q}H_2}]\left(\frac{k_0}{\alpha_3}\right) - [\mathrm{D\bar{Q}}]\left(\frac{V_{\max}}{K_{\mathrm{ma}} + [\mathrm{D\bar{Q}}]}\right)$$

(11)

Given α_1 and α_3 calculated from the fractions of DQ and DQH_2 bound to BSA obtained by ultrafiltration[1], the identifiable model parameters under steady-state conditions are the maximum reduction rate constant $V_{\max}$ (μmol·min^{-1}); the apparent Michaelis-Menten constant K_{ma} (μM); and the tissue-mediated DQH_2 oxidation rate constant k_o (ml·min^{-1}).

Under conditions of no DQH_2 oxidation to DQ (i.e., $k_o = 0$), *Eqs. 10* and *11* simplify to the following uncoupled ordinary differential equations

$$\mathrm{WV}_c \frac{\partial[\mathrm{D\bar{Q}}]}{\partial \mathrm{x}} = -[\mathrm{D\bar{Q}}]\left(\frac{V_{\max}}{K_{\mathrm{ma}} + [\mathrm{D\bar{Q}}]}\right)$$

(12)

$$\mathrm{WV}_c \frac{\partial[\mathrm{D\bar{Q}H_2}]}{\partial \mathrm{x}} = [\mathrm{D\bar{Q}}]\left(\frac{V_{\max}}{K_{\mathrm{ma}} + [\mathrm{D\bar{Q}}]}\right)$$

(13)

Integrating both sides of *Eq. 12* from x = 0 to x = L results in *Eq. 14*, which relates the rate of DQ reduction, v (μmol·min^{-1}), to the steady-state venous effluent [DQ] and [DQH_2], $V_{\max}$, and K_{ma}.

$$v = \frac{V_{\max}\,[\mathrm{D\bar{Q}}]_{\log}}{K_{\mathrm{ma}}\,[\mathrm{D\bar{Q}}]_{\log}}$$

(14)

where v is calculated as the product of the effluent steady-state [DQH_2] during DQ infusion times perfusate flow rate.

$$[\mathrm{D\bar{Q}}]_{\log} = \frac{[\mathrm{D\bar{Q}}]_{\mathrm{in}} - [\mathrm{D\bar{Q}}]_{\mathrm{out}}}{\ln([\mathrm{D\bar{Q}}]_{\mathrm{in}}/[\mathrm{D\bar{Q}}]_{\mathrm{out}})}$$

(15)

where $[DQ]_{in}$ is effluent steady-state ([DQ] + [DQH_2]) and $[DQ]_{out}$ is effluent steady-state [DQ] during DQ infusion. $[D\bar{Q}]_{log}$, referred to as the log mean [DQ], is the effective [DQ] in the capillary region during DQ infusion since [DQ] decreases as it passes through the capillary region[1, 7]. Thus the values of $V_{\max}$ and K_{ma} can be estimated by fitting *Eq. 14* to v as a function of $[D\bar{Q}]_{log}$.

Effect of Hyperoxia on DQ Reduction Rate

In the presence of cyanide, DQ reduction rate, v, is equal to the steady-state rate of DQH_2 efflux during DQ infusion calculated as the product of the effluent steady-state [DQH_2] (Table 3) and perfusate flow rate. Figure 5 shows v as a function of $[D\bar{Q}]_{log}$ for normoxic and hyperoxic lungs. The values of $V_{\max}$

(μmol/min) and K_{ma} (μM) were determined by fitting *Eq. 14* to the data shown in Fig. 5. Table 5 shows that exposure to hyperoxia for 21 days significantly increased V_{max} by ~107% and K_{ma} by ~240% compared with normoxic lungs.

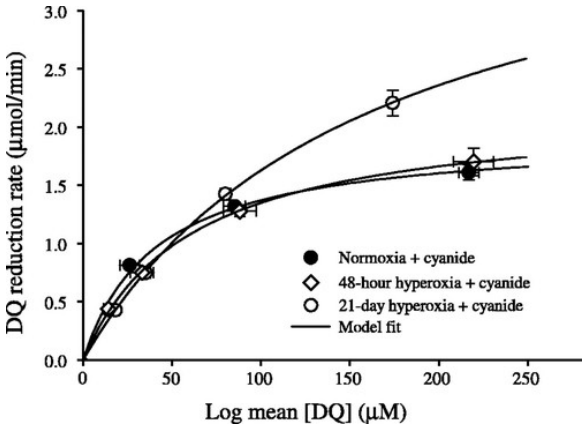

Fig. 5. The relationship between the rate of DQ reduction and the log mean [DQ] during DQ infusion in the presence of cyanide (2 mM) for normoxic and hyperoxic lungs. Values are means ± SE, *n* = 4, 3, and 4 for normoxic lungs, 48-h hyperoxic lungs, and 21-day hyperoxic lungs, respectively. Solid lines are fits of *Eq. 14* to the data.

Table 5. Kinetic parameters descriptive of DQ reduction to DQH_2 on passage through the lungs

	V_{max} (μmol/min)	K_{ma} (μM)
Normoxia	1.95±0.14	44±11
Hyperoxia, 48 h	2.13±0.12	58±6
Hyperoxia, 21 days	4.04±0.21*	149±11*

Values are means ± SE. V_{max} is the maximum rate of DQ reduction to DQH_2; K_{ma} is the apparent Michaelis-Menten constant for DQ reduction. For V_{max} and K_{ma}, *n* = 4, 3, and 4 for normoxic lungs, 48-h hyperoxic lungs, and 21-day hyperoxic lungs, respectively.
*Significantly different from the normoxic value.

Effects of Hyperoxia on DQH_2 Extravascular Volume, Vascular Volume, and Vascular Perfusion Heterogeneity

The extravascular volume of distribution accessible to DQH_2 (Q_D; ml), the vascular volume (Q_V; ml), and the relative dispersion of the vascular transit time distribution (RD_V) werecalculated from the data exemplified by Fig. 3 and FITC-dex tubing data (not shown) using the following equations

$$Q_v = F \times (t_R - t_T) \quad (16)$$

$$Q_D = F \times (t_D - t_R) \quad (17)$$

$$RD_v = \frac{\sqrt{(\sigma_R^2 - \sigma_T^2)}}{(t_R - t_T)} \quad (18)$$

where F is the perfusate flow rate (10 ml/min); t_R, t_D, and t_T are the respective mean transit times from bolus injection site to sample collection site for FITC-dex with the lung in place, (DQ + DQH_2) with the lung in place, and for FITC-dex with the lung removed; and are the variances of the concentration vs. times FITC-dex outflow curves with and without the lungs connected to the perfusion system, respectively. The different mean transit times and variances were estimated as previously described[3, 5]. The Q_D is a virtual volume that is equal to the product of a physical tissue volume and a tissue-to-perfusate partition coefficient[1]. Table 4 shows that exposure to hyperoxia for 21 days decreased Q_V by >30% and increased RD_V by >40% compared with normoxic lungs.

DISCUSSION

The results demonstrate that exposure to 85% O_2 for 21 days, but not for 48 h, increases lung capacity to reduce DQ to DQH_2. This increase is predominantly due to an increase in the rate of DQ reduction to DQH_2, with no significant effect on DQH_2 oxidation. The results also suggest that NQO1 is the dominant DQ reductase since DQ reduction was dicumarol inhibitable in normoxic and hyperoxic lungs. The increase in wet weights and wet/dry weight ratios of 21-day hyperoxic lungs had no significant effect on the extravascular volume accessible to DQH_2. As discussed next, these results are consistent with an increase in NQO1 activity in cells accessible to DQ from the vascular region in 21-day hyperoxic lungs.

Interpretation of the Increase in V_{max}, the Maximum Rate of DQ Reduction to DQH_2, in 21-Day Hyperoxic Lungs

In addition to increasing V_{max}, exposure of rats to hyperoxia for 21 days had increased lung dry weights (Table 1), consistent with an increase in their lung cellular content, presumably due to a large increase in the number of interstitial cells[14]. This brought into question whether the increase in V_{max} was simply the result of an increase in tissue mass (i.e., more cells) or an induction of NQO1 activity. As shown in Table 6, differences in the values of V_{max} can be accounted for by differences in lung dry weights (Table 1). However, normalization to lung dry weight assumes that all lung cells are accessible to DQ on passage through the pulmonary circulation. This would necessitate an increase in the extravascular volume accessible to DQH_2, Q_D, in 21-day hyperoxic lungs proportional to the increase in their dry weights, wherein Q_D is a measure of tissue volume accessible to lipophilic indicators such as DQ and DQH_2. However, the estimated values of Q_D for normoxic and hyperoxic lungs were not significantly different (Table 4), and hence the values of V_{max}/Q_D for 21-day hyperoxic lungs are larger than those for normoxic lungs (Table 6). These results are consistent with a hyperoxia-induced increase in NQO1 activity in cells accessible to DQ on passage through 21-day hyperoxic lungs, presumably dominated by capillary endothelial cells as discussed later.

Table 6. Normalized values of DQ maximum reduction rate, lung homogenate NQO1 activity

	V_{max}/Dry Wt (μmol·min^{-1}·g^{-1} wet wt)	**V_{max}/PS (μmol/ml)**	**V_{max}/Q_D (μmol·min^{-1}·ml^{-1})**	**Homogenate NQO1 Activity (nmol·min^{-1}·mg protein^{-1})**
Normoxia	8.5±0.6	0.089±0.006	1.69±0.12	452±17
Hyperoxia, 48 h	9.3±0.5	0.085±0.005	1.78±0.10	525±41
Hyperoxia, 21 days	10.5±0.6	0.697±0.037*	3.13±0.16*	607±60*

Values are means ± SE. V_{max} is the maximum rate of DQ reduction to DQH_2; PS is a measure of the rate constant of angiotensin converting enzyme-mediated FAPGG hydrolysis; Q_D is the lung DQH_2 extravascular volume; lung homogenate NAD(D)H:quinone oxidoreductase 1 (NQO1) activity is equal to the dicumarol-inhibitable 2,6-dichlorophenolinolophenol reduction rate. V_{max} values were normalized to the mean values of lung dry weights, PS, and Q_D values in Tables 1 and 5. For the normalized V_{max} values, *n* = 4, 3, and 4 for normoxic lungs, 48-h hyperoxic lungs, and 21-day hyperoxic lungs, respectively. For lung homogenate NQO1 activity, *n* = 5, 7, and 6 for normoxic lungs, 48-h hyperoxic lungs, and 21-day hyperoxic lungs, respectively.
*Significantly different from the normoxic value.

The extravascular volume of DQ was not determined since that would require perfusing the lung with 400 μM dicumarol to inhibit DQ reduction. This concentration of dicumarol would interfere with our ability to determine DQ venous effluent concentration spectrophotometrically due to the overlap between the DQ and dicumarol absorbance spectra. Because both DQ and DQH_2 are highly lipophilic and have flow-limited access to lung tissue, Q_D for DQH_2 can be thought of as an index of lung tissue volume accessible to lipophilic indicators such as DQ and DQH_2. Hence, a condition (hyperoxia) that changes Q_D for DQH_2 would be expected to also proportionately change Q_D for DQ.

The present study revealed a small increase (<9%) in wet/dry weight ratio of 21-day hyperoxic lungs compared with normoxic lungs indicating slight edema caused by chronic exposure to hyperoxia and/or perfusion. The kinetic model described in *Data Analysis* suggests that edema would be expected to increase Q_D, which would result in underestimating the increase in the value of V_{max}/Q_D for hyperoxic lungs (Table 6). Thus the estimated changes in the values of V_{max}/Q_D in Table 6 represent lower bounds on the impact of hyperoxia.

Exposure to hyperoxia for 21 days decreased the PS, which is a measure of the rate constant of ACE-mediated FAPGG hydrolysis (Table 4). Assuming that exposure to hyperoxia for 21 days had no significant effect on ACE activity per unit of surface area, this change in PS can be attributed to a change in perfused capillary surface area[27]. The decrease in PS (70% in 21-day hyperoxic lungs) is in fact consistent with the ~60% decrease in pulmonary capillary endothelial surface area in rats following exposure to 85% O_2 for 14 days measured morphometrically[14]. Normalizing V_{max} to PS results in an eightfold increase in NQO1 activity per unit of capillary surface area (Table 6). The loss of capillary endothelial surface area in 21-day hyperoxic lungs is not reflected by a change in DQH_2 extravascular volume (Table 4), which may suggest that nonendothelial cell types are also accessible to DQH_2. Alternatively, Crapo et al.[14] demonstrated that endothelial cells in lungs of rats exposed to 85% O_2 for 14 days undergo hypertrophy, with the net result of no change in the total volume of capillary endothelial cells.

The ~34% increase in lung homogenate NQO1 activity in 21-day hyperoxic lungs is less than one-half the ~85% increase in V_{max}/Q_D (Table 6), which can be taken as a measure of NQO1 activity per unit volume of lung cells accessible to DQ. One reason for this difference may be the complex nature of lung tissue and the additional complexity associated with the cellular changes in lungs of hyperoxia-adapted rats, including the increase in the number of interstitial cells[14]. Another possible reason is that key aspects of the intact lung environment that may regulate enzyme activity (e.g., the availability of electron donors and their accessibility to the enzyme) are not preserved in lung homogenate.

Interpretation of the Increase in K_{ma}, the Michaelis-Menten Constant for DQ Reduction to DQH_2, in 21-Day Hyperoxic Lungs

Because dicumarol has been shown to inhibit other reductases[28], one possible explanation for an increase in K_{ma} in 21-day hyperoxic lungs (Table 5) might be that dicumarol-inhibitable DQ reductase(s) other than NQO1 are induced.

Another possible explanation is an increase in the capillary transit time heterogeneity in 21-day hyperoxic lungs. The kinetic model described in *Data Analysis* assumes homogeneous transit time distribution. Table 4 shows that the RD_V in 21-day hyperoxic lungs increased by >40%. Most of the pulmonary vascular transit time heterogeneity is attributed to capillary transit time distribution [$h_c(t)$] [1, 5]. The kinetic model described in *Data Analysis* was used to evaluate the effects of $h_c(t)$ on V_{max} and K_{ma} values estimated under the assumption of homogeneous capillary transit times (*Eq. 14*) as described below.

A whole organ model that accounts for $h_c(t)$ was constructed based on the single capillary element model described in *Data Analysis*[5]. For the analysis, $h_c(t)$ was approximated using a random walk function and was accounted for in the whole organ model as previously described[1, 5]. To evaluate the effects of $h_c(t)$ on the estimated values of V_{max} and K_{ma}, two organ models were created to simulate DQ reduction on passage through normoxic lungs (normoxic model) and 21-day hyperoxic lungs (hyperoxic model). For the normoxic model, V_{max} was set at 2.0 µmol/min (Table 5); the relative dispersion of $h_c(t)$, RD_c, was set at 0.7 (Table 4); and K_{ma} was set at 10 µM, which was determined to result in a K_{ma} value estimated using *Eq. 14* equal to that for normoxic lungs (Table 5). For the hyperoxic model, V_{max} was set at 4.0 µmol/min (Table 5); RD_c was set at 1.0 (Table 4); and K_{ma} was set at the same value as for the normoxic model since K_{ma} is an intensive property of NQO1 and would not be expected to be affected by exposure to hyperoxia. The tissue-mediated DQH_2 oxidation rate constant, k_o, was set at zero for the normoxic and hyperoxic models to simulate lung perfusion with cyanide. For each model, DQ pulse infusions at 50, 100, 200, and 400 µM were simulated, and steady-state venous effluent [DQ] and [DQH_2] were determined. Figure 6 shows simulated steady-state rates of DQ reduction to DQH_2 as a function of the vascular log mean [DQ], $[D\bar{Q}]_{log}$. The differences between normoxic and hyperoxic models in Fig. 6 are nearly identical to those between the corresponding data in normoxic lungs and 21-day hyperoxic lungs (Fig. 5). The steady-state rates of DQ reduction (Fig. 6) for the hyperoxic model were larger than those for the normoxic model during the infusion of DQ at 200 and 400 µM, but not at 100 and 50 µM, consistent with an increase in K_{ma}. Table 7 shows the values of V_{max} and K_{ma} estimated by fitting *Eq. 14* to the simulated DQ reduction rates in Fig. 6 and designated "recovered values," normalized to the corresponding values used in the model simulations and designated "actual values." For V_{max}, the recovered values were within 10% of the actual values and were not sensitive to the relative dispersion of $h_c(t)$, RD_c. However, for K_{ma}, the recovered values for normoxic and hyperoxic models were more than 5-fold and 11-fold larger than the actual value, respectively. Thus the recovered K_{ma} value for the hyperoxic model was more than double that for the normoxic model, although the actual value was the same for both. This suggests that K_{ma} is sensitive to an increase in RD_c, which could account for the increase in K_{ma} in 21-day hyperoxic lungs compared with normoxic lungs (Table 5).

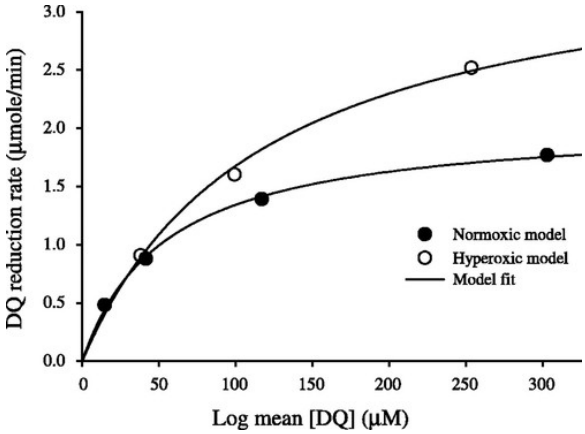

Fig. 6. The relationship between the rate of DQ reduction and the log mean [DQ] obtained from model-simulated infusions of DQ at 4 different concentrations (50, 100, 200, and 400 µM). The normoxic and hyperoxic whole organ models simulate DQ reduction on passage through normoxic and 21-day hyperoxic lungs, respectively. The whole organ models account for capillary transit time distribution, $h_c(t)$, and assume different relative dispersions for $h_c(t)$ (see text). Solid lines are fits of *Eq. 14* to simulation data. *Equation 14* assumes homogenous $h_c(t)$.

Table 7. The influence of capillary transit time distribution on the estimated values of $V_{\max}$ and K_{ma} from model simulations

	RD_c	**Recovered $V_{\max}$**	**Recovered K_{ma}**
		Actual $V_{\max}$	**Actual K_{ma}**
Normoxic model	0.7	1.04	5.4
Hyperoxic model	1.0	0.91	11.8

Normoxic and hyperoxic models simulate DQ reduction on passage through normoxic and 21-day hyperoxic lungs, respectively. $V_{\max}$ is the maximum rate of DQ reduction to DQH_2; RD_c is the relative dispersion of the capillary transit time distribution, $h_c(t)$; K_{ma} is the apparent Michaelis-Menten constant for DQ reduction. The values of $V_{\max}$ and K_{ma} estimated by fitting *Eq. 14* to the simulated DQ reduction rates in Fig. 6 are designated "recovered values." The $V_{\max}$ and K_{ma} values used in the model simulations are designated "actual values."

The above simulation results are consistent with those of Bass and Robinson[7]. They demonstrated that the effect of $h_c(t)$ on Michaelis-Menten kinetics is different for different regions of the substrate input concentration range, with its effect being insignificant for high input substrate concentrations compared with the Michaelis-Menten constant (zero order kinetics) since enzyme molecules in all capillaries are saturated by substrate. Hence, $V_{\max}$, which is determined mainly by DQ reduction rates at high-input DQ concentrations (relative to Michaelis-Menten constant), is virtually insensitive to $h_c(t)$, whereas K_{ma}, which is determined by reduction rates at low- and high-DQ input concentrations, is sensitive to $h_c(t)$.

The pulmonary capillary endothelium with its large surface area and direct contact with the perfusate might be expected to be the dominant site of DQ reduction in lungs. Previously, we demonstrated that bovine pulmonary artery endothelial cells in culture are capable of reducing DQ at a rate per cm^2 endothelial cell surface area comparable to that measured in lungs of normoxic rats [0.28 nmol/min per cm^2 endothelial surface area vs. 0.43 nmol/min per cm^2 in the present study, assuming a rat lung capillary surface area of ~4,500 cm^2 [14]][24]. On the basis of the fraction of DQ bound to BSA (~96% at 5% BSA)[1], the corresponding free K_{ma} value for DQ reduction in normoxic lungs is ~1.8 µM, which is also

consistent with 1.2 μM estimated by our previous studies[24] (Table 2). These results and the fact that the DQ reduction by the cultured pulmonary endothelial cells was dicumarol inhibitable are consistent with the pulmonary endothelium being a dominant site of DQ reduction in lungs. This is potentially important since the pulmonary capillary endothelium is primary target of O_2 toxicity and since NQO1 has been shown to confer protection from oxidant stress[8, 9, 17, 30, 31, 33].

The hyperoxia-induced increase in lung NQO1 activity may also have an impact on systemic organs by altering the redox status of compounds (e.g., quinones) passing through the lungs in preparation for entry into the systemic circulation. Depending on the physical and chemical properties of these compounds, the increase in lung NQO1 activity could represent an increased capacity to regenerate plasma antioxidants or production of prooxidant activity with potentially important implications for the physiology and pathophysiology of the systemic vascular system[1, 5, 10, 24].

GRANTS

This work was supported by National Heart, Lung, and Blood Institute Grants HL-24349 and HL-65537 and the Department of Veterans Affairs.

FOOTNOTES

- The costs of publication of this article were defrayed in part by the payment of page charges. The article must therefore be hereby marked "*advertisement*" in accordance with 18 U.S.C. Section 1734 solely to indicate this fact.

References

1. Audi SH**, Bongard RD, Dawson CA, Siegel D, Roerig DL, and Merker MP.** Duroquinone reduction during passage through the pulmonary circulation. ***Am J Physiol Lung Cell Mol Physiol*** *285*: L1116–L1131, 2003.
2. Audi SH**, Bongard RD, Okamoto Y, Merker MP, Roerig DL, and Dawson CA.** Pulmonary reduction of an intravascular redox polymer. ***Am J Physiol Lung Cell Mol Physiol*** *280*: L1290–L1299, 2001.
3. Audi SH**, Dawson CA, Ahlf SB, and Roerig DL.** Lung tissue mitochondrial benzodiazepine receptors increase in a model of pulmonary inflammation. ***Lung*** *180*: 241–250, 2002.
4. Audi SH**, Dawson CA, Ahlf SB, and Roerig DL.** Oxygen dependency of monoamine oxidase activity in the intact lung. ***Am J Physiol Lung Cell Mol Physiol*** *281*: L969–L981, 2001.
5. Audi SH**, Linehan JH, Krenz GS, and Dawson CA.** Accounting for the heterogeneity of capillary transit times in modeling multiple indicator dilution data. ***Ann Biomed Eng*** *26*: 914–930, 1998.
6. Audi SH**, Olson LE, Bongard RD, Roerig DL, Schulte ML, and Dawson CA.** Toluidine blue O and methylene blue as endothelial redox probes in the intact lung. ***Am J Physiol Heart Circ Physiol*** *278*: H137–H150, 2000.
7. Bass L **and Robinson PJ.** Effects of capillary heterogeneity on rates of steady uptake of substances by the intact liver. ***Microvasc Res*** *22*: 43–57, 1981.
8. Beyer RE**, Segura-Aguilar J, Di Bernardo S, Cavazzoni M, Fato R, Fiorentini D, Galli MC, Setti M, Landi L, and Lenaz G.** The role of DT-diaphorase in the maintenance of the reduced antioxidant form of coenzyme Q in membrane systems. ***Proc Natl Acad Sci USA*** *93*: 2528–2532, 1996.

9. Cadenas E**.** Antioxidant and prooxidant functions of DT-diaphorase in quinone metabolism. ***Biochem Pharmacol*** *49*: 127–140, 1995.
10. Cadenas E**, Boveris A, Ragan CI, and Stoppani AO.** Production of superoxide radicals and hydrogen peroxide by NADH-ubiquinone reductase and ubiquinol-cytochrome *c* reductase from beef-heart mitochondria. ***Arch Biochem Biophys*** *180*: 248–257, 1977.
11. Chang LY**, Kang BH, Slot JW, Vincent R, and Crapo JD.** Immunocytochemical localization of the sites of superoxide dismutase induction by hyperoxia in rat lungs. ***Lab Invest*** *73*: 29–39, 1995.
12. Cho HY**, Jedlicka AE, Reddy SP, Kensler TW, Yamamoto M, Zhang LY, and Kleeberger SR.** Role of NRF2 in protection against hyperoxic lung injury in mice. ***Am J Respir Cell Mol Biol*** *26*: 175–182, 2002.
13. Coursin DB**, Cihla HP, Will JA, and McCreary JL.** Adaptation to chronic hyperoxia. Biochemical effects and the response to subsequent lethal hyperoxia. ***Am Rev Respir Dis*** *135*: 1002–1006, 1987.
14. Crapo JD**, Barry BE, Foscue HA, and Shelburne J.** Structural and biochemical changes in rat lungs occurring during exposures to lethal and adaptive doses of oxygen. ***Am Rev Respir Dis*** *122*: 123–143, 1980.
15. Crapo JD **and Tierney DF.** Superoxide dismutase and pulmonary oxygen toxicity. ***Am J Physiol*** *226*: 1401–1407, 1974.
16. Cross CE**, Halliwell B, Borish ET, Pryor WA, Ames BN, Saul RL, McCord JM, and Harman D.** Oxygen radicals and human disease. ***Ann Intern Med*** *107*: 526–545, 1987.
17. Dinkova-Kostova AT **and Talalay P.** Persuasive evidence that quinone reductase type 1 (DT diaphorase) protects cells against the toxicity of electrophiles and reactive forms of oxygen. ***Free Radic Biol Med*** *29*: 231–240, 2000.
18. Forman HJ **and Fisher AB.** Antioxidant enzymes of rat granular pneumocytes. Constitutive levels and effect of hyperoxia. ***Lab Invest*** *45*: 1–6, 1981.
19. Halliwell B**.** ***Free Radicals in Biology and Medicine***. New York: Oxford, 1999.
20. Ho YS**.** Transgenic and knockout models for studying the role of lung antioxidant enzymes in defense against hyperoxia. ***Am J Respir Crit Care Med*** *166*: S51–S56, 2002.
21. Ho YS**, Dey MS, and Crapo JD.** Antioxidant enzyme expression in rat lungs during hyperoxia. ***Am J Physiol Lung Cell Mol Physiol*** *270*: L810–L818, 1996.
22. Lind C**, Cadenas E, Hochstein P, and Ernster L.** DTdiaphorase: purification, properties, and function. ***Methods Enzymol*** *186*: 287–301, 1990.
23. Ma Q**, Cui K, Wang RW, Lu AY, and Yang CS.** Site-directed mutagenesis of rat liver NAD(P)H: quinone oxidoreductase: roles of lysine 76 and cysteine 179. ***Arch Biochem Biophys*** *294*: 434–439, 1992.
24. Merker MP**, Bongard RD, Krenz GS, Zhao H, Fernandes VS, Kalyanaraman B, Hogg N, and Audi SH.** Impact of pulmonary arterial endothelial cells on duroquinone redox status. ***Free Radic Biol Med*** *37*: 86–103, 2004.
25. O'Donnell VB**, Smith GC, and Jones OT.** Involvement of phenyl radicals in iodonium inhibition of flavoenzymes. ***Mol Pharmacol*** *46*: 778–785, 1994.
26. Otterbein LE **and Choi AM.** The saga of leucine zippers continues: in response to oxidative stress. ***Am J Respir Cell Mol Biol*** *26*: 161–163, 2002.

27. Pitt BR**, Lister G, Davies P, and Reid LM.** Effects of changes in pulmonary perfusion and surface area on endothelial ACE activity. ***Ann Biomed Eng*** *15*: 229–238, 1987.
28. Ross D**, Siegel D, Beall H, Prakash AS, Mulcahy RT, and Gibson NW.** DT-diaphorase in activation and detoxification of quinones. Bioreductive activation of mitomycin C. ***Cancer Metastasis Rev*** *12*: 83–101, 1993.
29. Siegel D**, Franklin WA, and Ross D.** Immunohistochemical detection of NAD(P)H:quinone oxidoreductase in human lung and lung tumors. ***Clin Cancer Res*** *4*: 2065–2070, 1998.
30. Siegel D**, Gustafson DL, Dehn DL, Han JY, Boonchoong P, Berliner LJ, and Ross D.** NAD(P)H:quinone oxidoreductase 1: role as a superoxide scavenger. ***Mol Pharmacol*** *65*: 1238–1247, 2004.
31. Siegel D **and Ross D.** Immunodetection of NAD(P)H:quinone oxidoreductase 1 (NQO1) in human tissues. ***Free Radic Biol Med*** *29*: 246–253, 2000.
32. Wang Y**, Feinstein SI, Manevich Y, Ho YS, and Fisher AB.** Lung injury and mortality with hyperoxia are increased in peroxiredoxin 6 gene-targeted mice. ***Free Radic Biol Med*** *37*: 1736–1743, 2004.
33. Whitney PL **and Frank L.** Does lung NAD(P)H:quinone reductase (DT-diaphorase) play an antioxidant enzyme role in protection from hyperoxia? ***Biochim Biophys Acta*** *1156*: 275–282, 1993.
34. Wosilait WD**, Ryan MP, and Byington KH.** Uptake of anticoagulants by isolated rat hepatocytes. ***Drug Metab Dispos*** *9*: 80–84, 1981.